

Real-Time Fluorescence Detection of Multiple Microscale Cell Culture Analog Devices *In Situ*

Taek-il Oh,¹ Jong Hwan Sung,² Daniel A. Tatosian,² Michael L. Shuler,² Donghyun Kim^{1*}

¹School of Electrical and Electronic Engineering, Yonsei University, Seoul 120-749, Korea

²School of Chemical and Biomolecular Engineering, Cornell University, Ithaca, New York 14850

Received 10 April 2007; Revision Received 30 April 2007; Accepted 3 May 2007

Grant sponsor: National Core Research Center for Nanomedical Technology (KOSEF); Grant number: R15-2004-024-00000-0; Grant sponsor: Korea Research Foundation, Korean Government (MOEHRD); Grant number: KRF-2005-042-D00115; Grant sponsors: New York State Office of Science, Technology and Academic Research (NYSTAR) Program and by the National Science Foundation; Grant numbers: BES 0342985 and INT 0090356; Grant sponsor: National Science Foundation; Grant number: ECS-9731293.

*Correspondence to: Donghyun Kim, School of Electrical and Electronic Engineering, Yonsei University, Seoul 120-749, Korea.

Email: kimd@yonsei.ac.kr

Published online 8 June 2007 in Wiley InterScience (www.interscience.wiley.com)

DOI: 10.1002/cyto.a.20427

© 2007 International Society for Analytical Cytology

• Abstract

We investigated multiple microscale cell culture analog (μ CCA) assays *in situ* with a high-throughput imaging system that provides quantitative, nondestructive, and real-time data on cell viability. Since samples do not move between measurements, captured images allow accurate time-course measurements of cell population response and tracking the fate of each cell type on a quantitative basis. The optical system was evaluated by measuring the short-term response to ethanol exposure and long-term growth of drug-resistant tumor cell lines with simultaneous samples. The optical system based on epi-fluorescent excitation consists of an LED and a CCD as well as discrete optical components for imaging a large number of cells simultaneously. HepG2/C3A and MESSA cell lines were cultured in two μ CCA systems for continuous cell status monitoring in cell death experiments with ethanol and long-term cell growth. The experiment that tested ethanol uptake showed that ethanol immediately caused cell death. The system was applied to extracting dynamic constants in the uptake process. In the long-term cell growth experiment, growth of MESSA cells was followed by a stationary phase and eventual cell death attributed to nutrient and oxygen depletion and a change in the pH because of the accumulation of wastes by cell metabolism. HepG2/C3A cells were subject to contact inhibition and cell number did not change significantly over time. Issues related to long-term assays are also discussed. The quantitative results have been consistent with qualitative images and confirm the applicability of the portable optical system, and potential application to high-throughput analysis of cell-based assays to measure long-term dynamics. © 2007 International Society for Analytical Cytology

• Key terms

fluorescence detection; high-throughput screening; microscale cell culture analog; live cell imaging; cell status monitoring; green-fluorescent protein; cell dynamics

A cell culture analog (CCA) device is a cell-based assay using interconnected compartments with different cell type and can be used to evaluate toxicity and efficacy of various pharmacological agents (1). Using the well-established semiconductor microfabrication technology, a microscale cell culture analog (μ CCA) is fabricated from a silicon wafer. It consists of separate chambers for representing key organs in the human body, which are connected by microfluidic channels. The sizes of chambers and channels are designed so that they give similar residence times and liquid-to-cell ratios to the physiological values in the human body. A μ CCA system has an advantage that it can mimic animal tissue dimensions more realistically than larger tissue culture vessels. This technology has been previously shown to replicate toxicological events that are undetectable using ordinary *in vitro* experiments (2,3). Microfluidic-based cell chips such as the μ CCA presented in this paper are expected to provide a tool to decrease the time and cost of the drug discovery process especially in the phase prior to animal tests, because of its potential for high-throughput screening (4–6).

Typical viability tests on a μ CCA chip, similar to those on other types of cell-based assays, are performed with conventional epi-fluorescence microscopy. After running a toxicological test for 24 or 48 h, cells are stained with appropriate dyes. Fluorescence images are then acquired with a standard fluorescence microscope. For

live cells, fluorescence dyes that can track live cells without significantly affecting cell metabolism can be employed. Furthermore, there have been growing interests in inducible fluorescent gene products such as green fluorescent protein (GFP) (7–9). By counting the number of cells that are viable in a given field of view, one can determine the efficacy of a chemotherapeutic or similar drug *in vitro*.

In this procedure, however, the location on the chip where an image is taken differs for each image, which can cause substantial statistical variance and possibly influence the overall conclusion of a study. While multiple assay samples can be simultaneously tested to reduce the statistical variation, the deviation can remain considerable. In addition, obtained information about the cell status during an experiment is limited, because of the difficulties of making measurements multiple times without disconnecting the microfluidic system from a separate pump.

An incubating chamber with an optical window for live cell imaging may resolve these issues, for it may be made compact enough to fit into a standard microscope and contain an assay for *in situ* measurement. A microscope is sometimes integrated to enclose an incubating chamber. A good example is Ultraview™ of Perkin Elmer that is a confocal microscope mechanically integrated with an incubator (10). However, use of an incubating chamber, in addition to significantly increased hardware costs, is inappropriate for high-throughput analysis of a large number of μ CCAs, because an incubating chamber can house only a limited number of sample assays.

Our approach to tackle these issues is to develop a portable fluorescence-based optical microscope system and to perform *in situ* fluorescence measurements inside a standard incubator to investigate cellular response to a chemical. Since samples do not have to move between measurements, captured images allow more accurate time-course measurements of cell population response and, by doing so, tracking the fate of each cell type on a quantitative basis. Furthermore, cell viability is less affected by the movement itself. The system consists of discrete optical components such as lenses, beam splitters, and filters for optimal imaging performance and can be adjusted flexibly for high-throughput analysis with reduced alignment issues. The system was previously used for the real-time detection of cellular status in a single μ CCA device (11). While our system may be a simple combination of a regular microscope and a microfluidic cell culturing device, the reduced overall size allows portability into the cell culture environment and flexibility for high-throughput screening. In the current study, we extend the fluorescence-based imaging system to investigate multiple μ CCAs for high-throughput screening. This indicates that the system measures test and control chips simultaneously in a single experiment. Results can be considered as being measured in the same conditions, so that the comparison between chips can be more substantive.

For an initial feasibility study, we have used a calcein acetoxymethylester (calcein AM) staining technique for quantitative analysis of cytotoxic uptake of ethanol (EtOH) over 3 h. Real-time experiments for a longer period are often complicated with issues such as cell division and long-term effective-

ness of fluorescence dye molecules. This observation motivated us to exploring the long-term applicability of the system by determining nutrient-limited cell growth curves in a μ CCA device for over 85 h on a continuous basis. The long-term measurement is based on the expression of enhanced GFP (EGFP), which has good photostability and thus is relatively insensitive to photobleaching for a large number of exposures for long-term observation (12).

MATERIALS AND METHODS

Optical System Design

Initially, we considered an all-optical design for multi-chip characterization without mechanical movement. Such a set-up; however, is subject to optical power reduction with $1/N$ (N : number of assays) as well as extra power loss involved in the use of additional optical components and an increasingly complicated design. Thus, the system we describe here is based on a mechanical motorized stage for imaging multiple μ CCA samples as well as multiple chambers within each μ CCA system. In the future, we believe that the system may benefit from optically performing multi-chamber imaging within a μ CCA sample.

The optical system, based on epi-fluorescence microscopy, is shown in Figure 1 and employs a high-power light emitting diode (LED) and a charge coupled device (CCD) camera, respectively, as a light source and a detector. The overall imaging system is designed to offer low magnification to provide cell status information on the basis of a statistical average by imaging a large number of cells simultaneously. Light from a high power royal blue LED (Luxeon LXHL-BR02, Philips, San Jose, CA) of peak wavelength at $\lambda = 455$ nm and optical power at 220 mW lumens (manufacturer provided) is focused by an imaging lens L1 ($f = 35$ mm, $d = 24.5$ mm) to excite EGFP and calcein AM on μ CCA samples. Excited fluorescence imaged by L1 is occasionally relayed by L2 ($f = 150$ mm, $d = 50$ mm), to a CCD (QICAM FAST 1394, Qimaging, Burnaby, BC, Canada). A pinhole aperture is placed for baffling out the noise from background. The center wavelength/

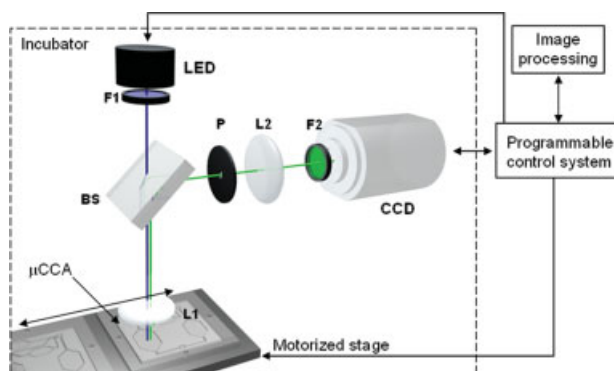


Figure 1. Detection system overview (F1: excitation filter, F2: emission filter, L1, imaging lens, L2: relay lens, P: pin-hole, and BS: beam splitter). The blue and green solid lines represent an illuminating and emitted beam, respectively. [Color figure can be viewed in the online issue, which is available at www.interscience.wiley.com.]

bandwidth of the excitation filter (F1) and emission filter (F2) in a fluorescence filter cube (31054GFP, Chroma Technology, Rockingham, VT) are given respectively by 455/70 nm and 525/30 nm (provided by the manufacturer). F1 blocks noncollimated Lambertian types of illumination from an LED. The intensity difference because of the Lambertian illumination can be ignored because the field of view ($\sim 500 \times 600 \mu\text{m}^2$) is much smaller than the illumination cone. If there remains background noise on the CCD due to possible stray light, illumination correction is performed in the image processing step. In addition, the effect of noncollimation through F2 is minimal because the sample-to-L1 distance is close to the focal length of L1 and thus the image distance from L1 is large relative to the overall size of the system. Two μCCA chips were mounted on a motorized stage (UTM100CC1DD, Newport, Irvine, CA) with a linear resolution of 1 μm (provided by the manufacturer). The total dimension of the optical system is 30(L) \times 23(W) \times 20(H) cm^3 . Potentially, the system can be made more compact to accommodate more μCCA chips.

The light source spectra have been measured by an optical spectrometer for calibration. Maximum power has been measured at $\lambda = 459.5 \text{ nm}$ with the full width-half maximum as 25 nm. Thus, slight discrepancy exists between measured and manufacturer provided peak wavelengths. The cutoff wavelength, defined as the wavelength at which the optical power is reduced to 1% of the maximum is 524 nm without using F1. This overlaps the emission spectrum of EGFP and calcein AM. When the excitation filter F1 is mounted on the LED, the cutoff wavelength is decreased to 498 nm, which removes the source interference due to excitation of fluorescence dyes. Using programmed control, μCCA samples have been exposed minimally at 0.7–1.6 s for each measurement to protect cells from getting photobleached (7).

Since a CCD is afflicted inherently with dark current noise, thermal noise characterization is required at an incubating temperature of 37°C (13,14). From an initial test of a CCD, the dark current noise has been determined to be saturated at a constant level 25 min after the system was installed in an incubator. The maximum change in the dark current noise is a 10% increase, compared to that of room temperature. Experimental measurements were initiated at least 30 min after a CCD was turned on.

The transition between chambers has been made mechanically. The transition time has been controlled to be short for minimal disparity between measurement conditions and yet sufficiently long to take observable time not to affect the drug diffusion process in μCCA . The transition time was 5–12 s, depending on the distance that a motorized stage traveled. Registration error of the motorized stage was less than 1 μm , which is far smaller than the cell size. Thus, misregistration in the images taken at different time points was minimal.

Cell Culture

The cell lines used in this study (HepG2/C3A and MESSA) were obtained from the American Type Culture Collection (ATCC, Manassas, VA) and modified further if necessary. All the cell lines were cultured in the appropri-

ate media recommended from ATCC, supplemented with 10% FBS from Invitrogen (Carlsbad, CA). Media used for culturing the cell lines were minimum essential medium (MEM) from Invitrogen and McCoy's 5a medium from Sigma Aldrich (St Louis, MO), respectively, for HepG2/C3A and MESSA cell lines. For all μCCA experiments, McCoy's 5a medium was used since it has higher composition of nutrients. Calcein AM was purchased from Invitrogen and ethanol from Sigma Aldrich.

Preparation of μCCA Assays

Fabrication of μCCA devices has been elaborated elsewhere (15). The μCCA used in this study is shown in Figure 2a and chambers are listed in Table 1. The liver hepatoma cell-

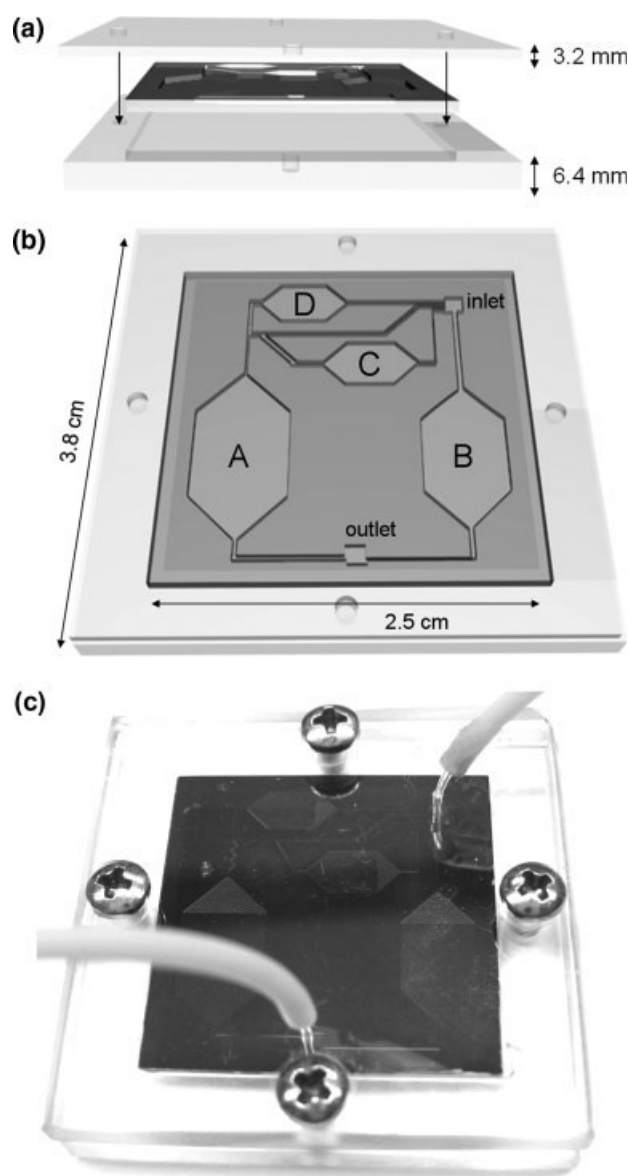


Figure 2. (a) Assembly of a μCCA device sealed with a PMMA holder and (b) its final form (A, B, C, and D for four compartments). (c) A μCCA device with silicone tubes.

Table 1. Chamber designation and dimensional parameters of the μ CCA chip under test

	LIVER (A)	UTERUS CANCER (B)	NORMAL COLON (C)	COLON TUMOR (D)
Width (mm)	7	6	4	4
Depth (μ m)	60	60	60	60
Area (mm ²)	61.3	45	20	20
Volume (μ l)	3.68	2.9	1.2	1.2

line HepG2/C3A is seeded on the liver chamber (A) and a cell line derived from uterine cancer, MESSA, was seeded on the uterus cancer chamber (B). The normal colon cell chamber (C) and colon tumor cell chamber (D) were not used in this study. Cells grow attached to the bottom surface of the chamber. To minimize autofluorescence of plastic packaging material, PMMA has been used as a top cover of μ CCA (16).

For the long-term growth study, MESSA and HepG2/C3A cell line transfected with H2B-GFP gene were used. The fusion protein H2B-GFP, which is a human histone protein fused at the amino terminus to EGFP. The histone protein binds to DNA and helps with opening and closing DNA strands during replication. It has previously been observed that the fluorescence of this protein is significantly reduced during cell death (17). Therefore, the viability of a cell can be determined by measuring the fluorescence intensity of the cell.

Chip preparation and CCA experiment protocol are described in detail elsewhere (15). To describe the steps briefly, the chips were immersed in piranha solution for 20 min to remove organic residues, and autoclaved for sterilization. Then the chips were coated with 0.1 mg/ml poly-D-lysine (Sigma-Aldrich), followed by washing with PBS and coating with 50 μ g/ml fibronectin (Chemicon International, Temecula, CA). Cells were trypsinized and resuspended in medium to the final concentration of 7.5×10^5 cells/ml. An appropriate volume of cell suspension (20–50 μ l) was placed on each chamber to completely cover the chamber without overflow. Chips loaded with cells were incubated at 37°C with 5% CO₂ overnight. In case it was necessary, the whole chip was stained with calcein AM to distinguish live cells. Before assembling the CCA device, whole chip was immersed in 2 μ M calcein AM solution for 30 min. Then the chips were assembled and sealed with a PMMA holder (Figs. 2a and 2b). Silicone tubes (PharMed Pump Tubing, inside diameter = 0.25 mm, Cole-Parmer, IL) were used to connect the assembled CCA with a medium reservoir as shown in Figure 2c. A peristaltic pump was used to supply the medium at a constant speed (0.5 rpm equivalent to 2 μ l/min approximately).

Cell Death Experiment with Ethanol

To verify that the optical system is capable of detecting the process of cell death in real-time, the cells in the CCA device were treated with various concentrations of ethanol. For this experiment, the cells on the chips were stained with calcein AM prior to the assembly of the CCA device. After setting up the CCA device and the optical system, initial measurements were made for 20 min while supplying media with

a peristaltic pump, in order to ensure that the cells were being monitored consistently. External reservoirs were prepared to contain various concentrations of ethanol (0–20% v/v) well-mixed in culture media. After 20 min passed, reservoirs were changed to have ethanol of target concentration flow into the system to induce a rapid cell death. The measurements were continued until there were no live cells detected, which took up to 120 min depending on the concentration of ethanol.

Long-Term Cell Growth Experiment

The long-term growth of cells in the CCA device was monitored with the optical system in order to verify that the system can be operated for several days while making real-time measurements. Cells transfected with H2B-GFP express GFP protein constitutively, thus giving off green fluorescent signal as long as they are live (17). The CCA chips loaded with both cells lines were assembled and the whole optical system with the CCA device and a peristaltic pump were put in an incubator which was kept at 37°C, 5% CO₂. For the long-term growth experiment, the CCA device was connected to a medium reservoir via silicone tubes, and the media coming out of the CCA device were fed back into the medium reservoir, therefore the media were being recirculated into the system for the whole time. The volume of the medium reservoir was 200 μ l, which supports the growth of cells for about three days, and the measurements were made for 85 h until the nutrients in the media became depleted and the accumulation of toxic wastes by cells eventually caused the cells to die.

Image Processing

Intensity graphs have been produced and cells counted from acquired fluorescence images using Cell ProfilerTM after several steps of removing the effect of background noise. The image processing using the software is described elsewhere (18–20). The steps involve cropping, illumination correction, thresholding, and measuring identified objects. The illumination correction is a step of correcting uneven light distribution across a field of view since the center of a field of view is more strongly illuminated. A precalculated illumination function is used to produce corrected images. Thresholding distinguishes signal from noise. In the case of EtOH tests, the threshold level was selected as approximately 30% of initial fluorescent intensity. The overall image processing can be performed based on object numbers, areas occupied by objects, and image intensity. Image processing based on these procedures, in general, provided consistent results.

RESULTS AND DISCUSSION

Since the portable fluorescent imaging system measures cells *in situ*, a sequence of fluorescence images can be quantified as intensity variation over time. The system has been applied to cell viability tests against a cytotoxic chemical by measuring changes of calcein AM signal and cell growth curves on μ CCA by measuring the intensity variation of EGFP of target cells cultured in multiple μ CCA systems. An overall pur-

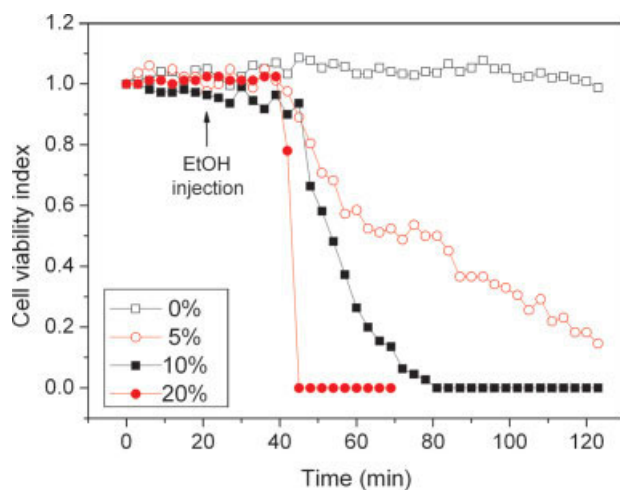


Figure 3. Variation of cell viability index after 0% (control), 5, 10, and 20% EtOH injection at 20th min. [Color figure can be viewed in the online issue, which is available at www.interscience.wiley.com.]

pose of these tests is to identify strengths and weaknesses of our imaging system that addresses cell-based assays for different time scales.

Cell Death Experiment with EtOH

The first set of experiments tested response to ethanol addition and was conducted on two identical μ CCA chips where HepG2/C3A cells were seeded and cultured under the same measurement conditions. Target HepG2/C3A cells were

treated with calcein AM for fluorescence detection prior to the packaging of μ CCA. The cytotoxicity of ethanol is well-known (21–23). Figure 3 shows the cell number variation in terms of cell viability index (CVI) measured in real-time. For consistent comparison of the cell growth and maintenance, CVI was defined as the ratio of the cell number at a specific time to the initial cell number. In other words, CVI measures relative increase or decrease in reference to the initial cell number. EtOH was injected 20 min after running the chips using a peristaltic pump. EtOH travels through the silicone tubes for approximately 21 min to reach a chamber. In other words, cells were exposed to EtOH at 41st min since the test chips were initially run, as shown in Figure 3. The graph shows that when the cells were exposed to ethanol, it immediately caused cell death, and all cells died within the time range of a few minutes to 1 h, depending on the applied EtOH concentration.

Figure 4 shows real-time fluorescence images of HepG2/C3A cells at EtOH concentration of 0% (top row), 5% (second row), 10% (third row), and 20% (bottom row). Figures 3 and 4 emphasize the strengths of our system to track the position of an individual cell and to observe cell dynamics quantitatively. A time constant τ can be associated with the cell death in response to EtOH. Namely, τ indicates the time it takes for cells to die at a specific EtOH concentration in a given experimental environment. τ depends on parameters such as chemical concentration, cell types, cell status, flow rates, etc. Figure 5 presents the necrosis time constant τ over different EtOH concentration values. Here, τ was obtained as a time constant that reaches CVI = 0.01 for cell death. More specifically, at 20% EtOH, HepG2/C3A cells die almost immediately with CVI reaching less than 0.01 at 2 min, while at 10% EtOH the CVI decreased to 0.01–30

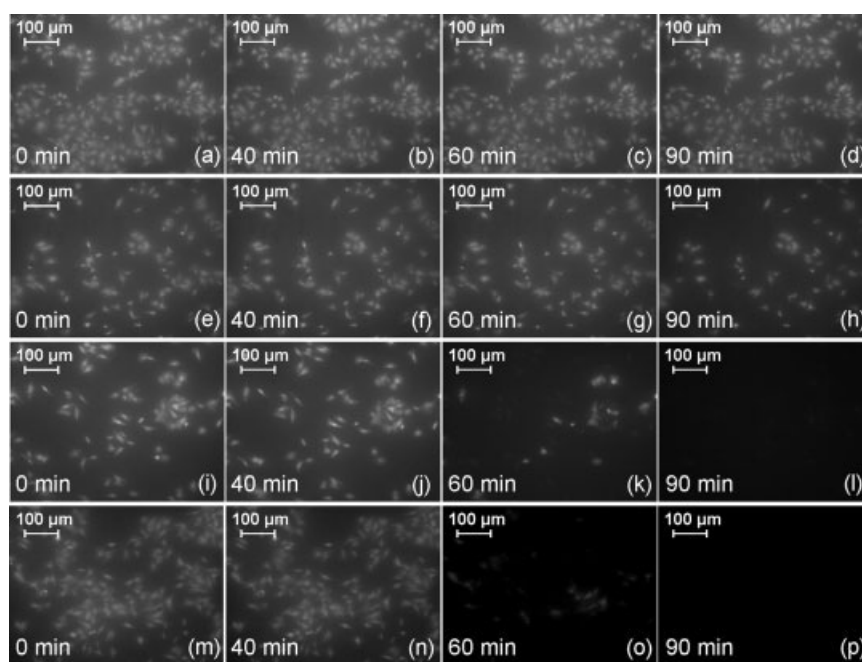


Figure 4. Fluorescence images of HepG2/C3A cells exposed to EtOH concentration of 0% (control, top row, a-d), 5% (second row, e-h), 10% (third row, i-l), and 20% (bottom row, m-p). EtOH was injected 20 min after the test was begun.

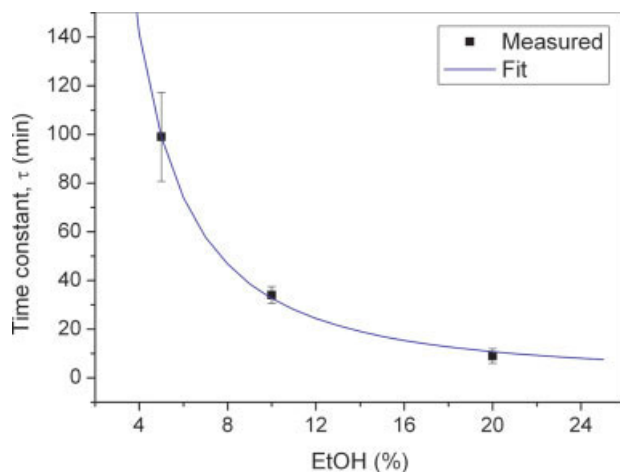


Figure 5. Cell death time constant τ at various EtOH concentration, fitted by $\tau = 1,300/C_{\text{EtOH}}^{1.6}$. [Color figure can be viewed in the online issue, which is available at www.interscience.wiley.com.]

min post the treatment. The 5% treatment reduced CVI to about 0.1 at 80 min post treatment. Figure 5 suggests that the dependence of τ on EtOH is not linear. Good correlation was achieved with an inverse relationship, i.e. $\tau(C_{\text{EtOH}}) = A/C_{\text{EtOH}}^n$, where C_{EtOH} denotes ethanol concentration. A and n are fitting constants and were determined as $A = 1,300$ and $n = 1.6$. Note that the elimination of blood EtOH is known to obey nonlinear kinetics (24). Generally, cell death experiments with cytotoxic agents show nonlinear dose responses. For example, tumor cells show dose-dependent increasing fractions of apoptosis in response to antitumor agents such as 5-FU (5-fluorouracil), Oxaliplatin and CTP-11 in a nonlinear manner (25). Also the growth rate of tumor cells is affected by the presence of cytotoxic chemicals in a dose-dependent manner, and the relationship between the dose of chemicals and the inhibition of growth is nonlinear (26).

As an extension of the first experiment, calcein AM was supplied by injecting it through microfluidic channels, instead of treating the cells with calcein AM prior to packaging μCCA

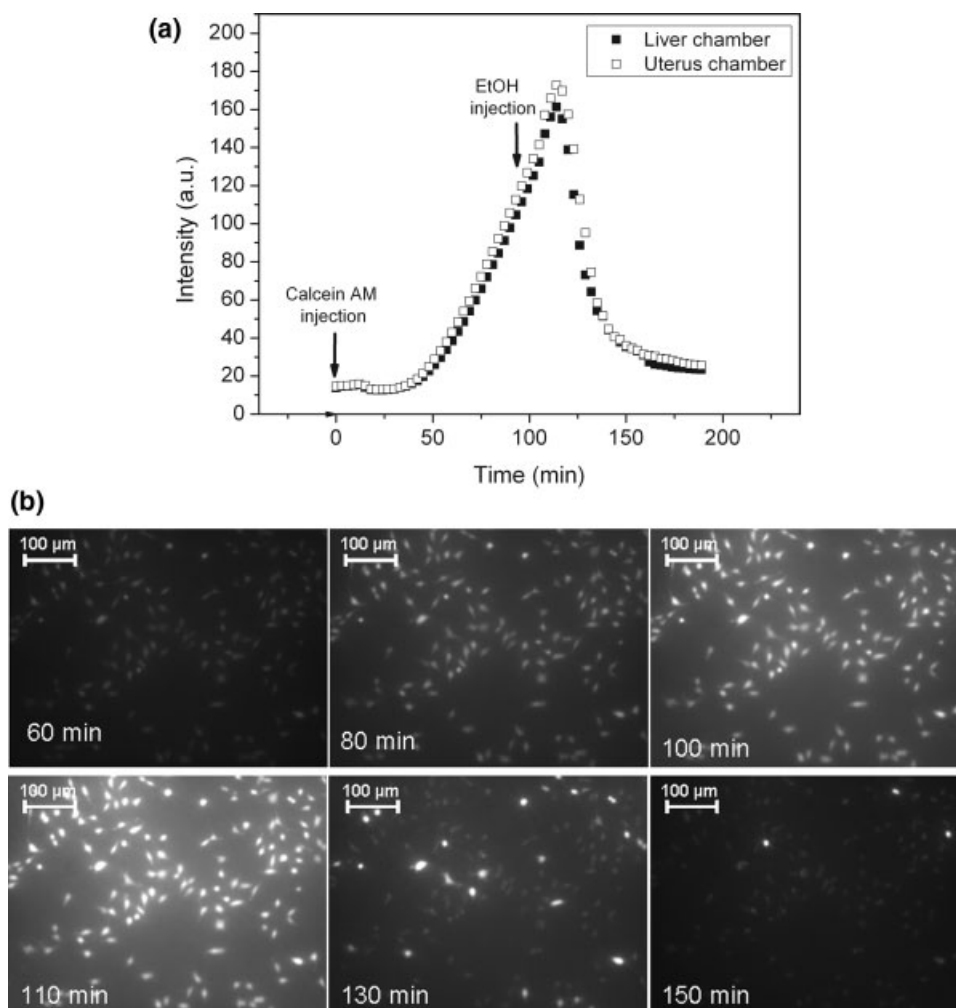


Figure 6. (a) Fluorescence intensity graph of HepG2/C3A cells in liver and uterus cancer chamber that shows initial calcein AM (2 μM , injected externally) uptake and following cytotoxicity of 10% EtOH injected at 90th min. (b) Corresponding fluorescence images of HepG2/C3A cells in the liver chamber.

chips. The main purpose of this change is to understand the dynamics of calcein AM staining in addition to EtOH when calcein AM is supplied externally after a sample is run. Results of intensity-based analysis presented in Figure 6a on HepG2/C3A cells show that the calcein AM fluorescence intensity increases until 10% EtOH was injected at 90th min and delivered through a tube to reach cells in each chamber. Because of the chemical toxicity of EtOH, the uptaken stain molecules of calcein AM barely stay inside the cells. While almost identical behavior of the fluorescent intensity was measured in different chambers, slight delay in the calcein uptake in the liver chamber can be associated with the difference in medium circulation paths as shown in Figure 2b. The delay is estimated to be approximately one temporal resolution long, which is 3 min. On the other hand, the strong toxicity of EtOH affects cells quickly enough to obliterate the difference in the fluorescence intensity effectively. Figure 6b shows fluorescent images that reflect on the dynamics of staining procedure and the fluorescence intensity change by EtOH. The maximum intensity was observed at 110th min while few cells remain visible after 150 min. The images presented in Figure 6b are in good agreement with the intensity-based data given quantitatively by Figure 6a.

Long-Term Cell Growth Experiment

The second experiment concerns the evaluation of the growth and maintenance of liver and tumor cells using two μ CCA chips. Typically, a cell growth curve on a μ CCA depends on many factors such as initial cell density, nutrient supply from reservoir, cell distribution, cell growth phase, and stress in a μ CCA (eg. hydrodynamic shear stress) (27). The growth curve of MESSA H2B-GFP cells in the chamber B of the first μ CCA chip has been obtained for an 85 h experiment (Fig. 7). In Figure 7, the growth and maintenance curve for MESSA H2B-GFP cells shows that cells start proliferating after an initial lag phase (about 30 h). Cells then grow until about 65th hour (from 0.95 to 1.33 a.u.) when they enter into a stationary phase. After the stationary phase, the cell number starts to decrease. The decrease in the cell number after 70 h reflects the fact that the cells die and detach from the surface. The death of cells can be attributed to nutrient and oxygen depletion, and a change in the pH because of the accumulation of wastes by cell metabolism.

Figure 7 also presents the cell growth and maintenance curve of HepG2/C3A H2B-GFP cells in the chamber A of the second μ CCA chip. Similar to CVI, cell growth index was defined for quantitative comparison as normalized cell number with respect to an initial cell number. The results show that HepG2/C3A H2B-GFP cells are subject to contact inhibition and cell number does not change significantly over time, compared to MESSA H2B-GFP. No growth was expected as the cells were seeded on the chip at high confluency. Consequently, the liver chamber was almost fully confluent when the experiment started. HepG2/C3A is a derivative cell-line of HepG2 cell-line, selected for strong contact inhibition of growth and high albumin production (28). The lack of space would be expected to prevent cell growth. Also, HepG2/C3A cell-line

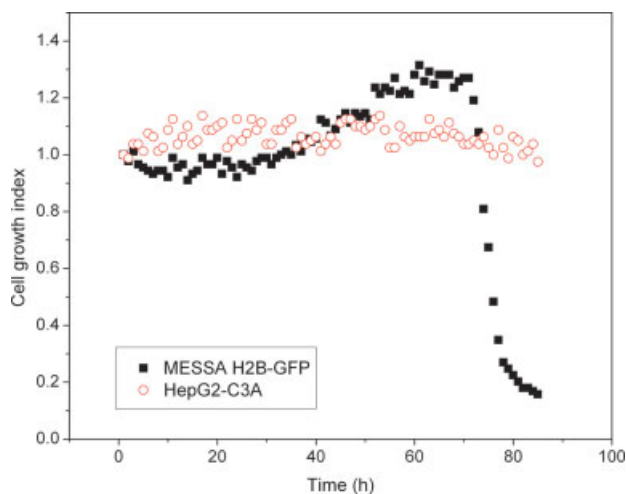


Figure 7. Cell growth index of MESSA H2B-GFP and HepG2/C3A cells in μ CCA assays. [Color figure can be viewed in the online issue, which is available at www.interscience.wiley.com.]

grows slower than MESSA H2B-GFP cells, which is a tumor cell-line. Note that liver cell division time is 32–35 h, compared with the division time of tumor cells, which is 22–24 h (29,30). If seeded at a low cell density, the growth of HepG2/C3A cells may be observed clearly, but the μ CCA experiments required nearly confluent cell layers.

The reason for seeding the cells at such a high density was to ensure that the cells made a good contact to the silicon surface, so that the cells could maintain their viability over a long period in the presence of hydrodynamic shear stress. When cells were seeded in a lower density and the flow was introduced, often cells seemed to be less healthy and less spread out, judging from the cell morphology under the microscope. It has been shown that the spreading and making a strong adhesion to the surface is important for the viability of cells (31,32). In the case of HepG2/C3A H2B-GFP cells, the cell number does not decrease significantly even after 80th h, although the decrease appears to start after about 55th h. This trend is associated with the nature of the HepG2/C3A cell-line that typically adheres to the surface more strongly than the tumor cell-line MESSA H2B-GFP. When HepG2/C3A cells are cultured in culture flasks and trypsinized for a subculture, they are rinsed with 0.25% (w/v) trypsin and 0.53 mM EDTA solution to remove all traces of serum. They generally require a longer incubation time with trypsin-EDTA than other tumor cell-lines until the cells detach from the surface (28). For an identical incubation time, HepG2/C3A cells likely adhered to the surface even at a critical stage where the tumor cells have already been detached. HepG2/C3A cells may also be more resistant to the stress conditions that inhibit MESSA H2B-GFP cells.

Figure 8 is fluorescence images of HepG2/C3A cells in chamber A and MESSA H2B-GFP cells in chamber B. As described earlier, the images shown in Figure 8 are in qualitative agreement with the quantitative data presented in Figure 7 so that no significant change is observed in the case of

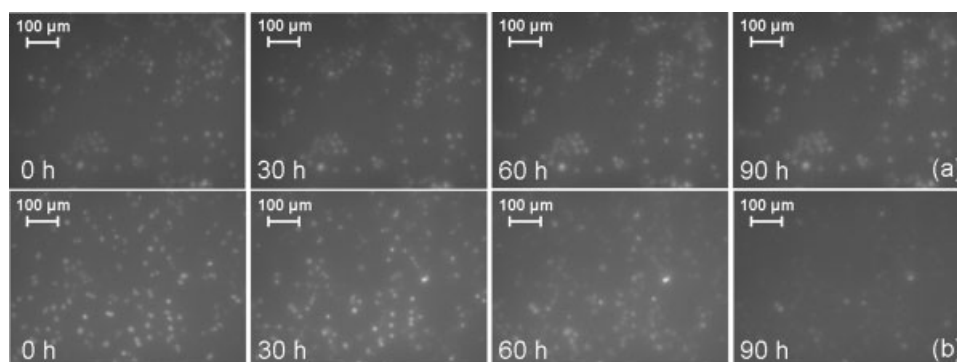


Figure 8. Cell growth fluorescence images of (a) HepG2/C3A cells in the chamber A and (b) MESSA H2B-GFP cells in the chamber B.

HepG2/C3A, while the cell number for MESSA H2B-GFP fluctuates until eventual cell death after 85 h.

In contrast to experiments with cell-based assays where measurements are made over a relatively short period of time, cells in long-term assays may undergo a number of cell mitoses that are often accompanied by cell detachment. Unlike static cell culture conditions, in a microfluidic environment mitotic cells can detach from the surface because of shear, therefore a quiescence state of cells can be obtained depending on the flow rate (33). This means that cell growth index tends to be underestimated as the period of an experiment becomes longer, which may partially explain why cell growth index in the case of HepG2/C3A cells does not grow significantly and relative mild increase for MESSA H2B-GFP cancer cells. Although quantitative evaluation of the extent of cell mitosis was not attempted in our study, our imaging system, with sufficient temporal resolution, can discriminate mitotic cells that are consequently detached. This is because it measures cells *in situ* and thus a surface attached individual cell can be traced on a morphological basis. For this reason, cell number-based analysis is more appropriate in considering cell detachment than intensity-based approach. In addition to increasing temporal resolution of *in situ* measurement, a study is currently under way to optimize the structure of μ CCA assays so that cell detachment as a result of mitosis can be minimized.

CONCLUDING REMARKS

In this study, we investigated an optical imaging system that makes measurements *in situ* of multiple μ CCA assays and provides quantitative data of the cell viability in real-time. The system was applied to measuring nutrient-limited cell growth for normal and tumor cell-lines and also to exploring the effects of EtOH on the HepG2/C3A cell-line using two μ CCA samples. We have estimated to extract dynamic constants involved in the uptake process out of measured data. Issues related to long-term measurement were also discussed. The quantitative results when monitoring cells for many hours have been consistent with qualitative images and confirm the applicability of the system especially for real-time high-throughput analysis of cell-based assays.

ACKNOWLEDGMENTS

The authors appreciate Glenn Swan for kindly building and providing hardware packaging for optical components. T. Oh thanks Jong-ryul Choi and also Kyung Hoon Yoon for helpful discussion.

LITERATURE CITED

- Shuler ML, Ghanem A, Quick D, Wong MC, Miller P. A self-regulating cell culture analog device to mimic animal and human toxicological responses. *Biotechnol Bioeng* 1996;52:45–60.
- Viravaidya K, Sin A, Shuler ML. Development of a microscale cell culture analog to probe naphthalene toxicity. *Biotechnol Prog* 2004;20:316–323.
- Viravaidya K, Shuler ML. Incorporation of 3T3-L1 cells to mimic bioaccumulation in a microscale cell culture analog device for toxicity studies. *Biotechnol Prog* 2004;20:590–597.
- Andersson H, van den Berg A. Microfabrication and microfluidics for tissue engineering: state of the art and future opportunities. *Lab Chip* 2004;4:98–103.
- El-Ali J, Sorger PK, Jensen KF. Cells on chips. *Nature* 2006;442:403–411.
- Pihl JM, Karlsson M, Chiu DT. Microfluidic technologies in drug discovery. *Drug Discovery Today* 2005;10:1377–1383.
- Stephens DJ, Allan VJ. Light microscopy techniques for live cell imaging. *Science* 2003;300:82–86.
- Yuste R. Fluorescence microscopy today. *Nature Methods* 2005;2:902–904.
- Lichtman JW, Conchello J-A. Fluorescence microscopy. *Nature Methods* 2005;2:910–919.
- Egner A, Andresen V, Hell SW. Comparison of the axial resolution of practical Nipkow-disk confocal fluorescence microscopy with that of multifocal multiphoton microscopy: Theory and experiment. *J Microsc* 2002;206:24–32.
- Tatosian DA, Shuler ML, Kim D. Portable in-situ fluorescence cytometry of microscale cell-based assay. *Opt Lett* 2005;30:1689–1691.
- Shaner NC, Steinbach PA, Tsien RY. A guide to choosing fluorescent proteins. *Nature Methods* 2005;2:905–909.
- Goldman RD, Spector DL. *Live Cell Imaging*. New York: Cold Spring Harbor Laboratory; 2005. pp 87–100.
- Lanza RC, Shi S, McFarland EW. A cooled CCD based neutron imaging system for low fluence neutron sources. *IEEE Trans Nucl Sci* 1996;43:1347–1351.
- Sin A, Chin KC, Jamil ME, Kostov Y, Rao G, Shuler ML. The design and fabrication of three-chamber microscale cell culture analog devices with integrated dissolved oxygen sensors. *Biotechnol Prog* 2004;20:338–345.
- Piruska A, Nikcevic I, Lee SH, Ahn C, Heineman WR, Limbach PA, Seliskar CJ. The autofluorescence of plastic materials and chips measured under laser irradiation. *Lab Chip* 2005;5:1348–1354.
- Gavrieli Y, Sherman Y, Ben-Sasson SA. Identification of programmed cell death in situ via specific labeling of nuclear DNA fragmentation. *J Cell Biol* 1992;119:493–501.
- Cell Profiler TM, Available at: <http://www.cellprofiler.org>.
- Lamprecht MR, Sabatini DM, Carpenter AE. CellProfiler™. Free, versatile software for automated biological image analysis. *BioTech* 2007;42:71–75.
- Carpenter AE, Jones TR, Lamprecht MR, Clarke C, Kang IH, Friman O, Guertin DA, Chang JH, Lindquist RA, Moffat J, Golland P, Sabatini DM. CellProfiler: image analysis software for identifying and quantifying cell phenotypes. *Genome Biol* 2006;7:R100.
- Chen S-Y, Yang B, Jacobson K, Sulik KK. The membrane disordering effect of ethanol on neural crest cells in vitro and the protective role of GM1 ganglioside. *Alcohol* 1996;13:589–595.
- Wan JY, Wang JY, Wang Y, Wang JY. A comparison between acute exposures to ethanol and acetaldehyde on neurotoxicity, nitric oxide production and NMDA-induced

- excitotoxicity in primary cultures of cortical neurons. *Chin J Physiol* 2000;43:131–138.
23. Mashimo K, Sato S, Ohno Y. Acute cytotoxic effects of ethanol on cultured mouse myocardial cells in a monolayer—Enzymatic, chronotropic and ultrastructural studies. *Jpn J Alcohol Studies Drug Dependence* 2001;36:142–153.
 24. Fujimiya T, Yamaoka K, Fukui Y. Parallel first-order and Michaelis-Menten elimination kinetics of ethanol. Respective role of alcohol dehydrogenase (ADH), non-ADH and first-order pathways. *J Pharmacol Exp Ther* 1989;249:311–317.
 25. Boyer J, McLean EG, Aroori S, Wilson P, McCulla A, Carey PD, Longley DB, Johnston PG. Characterization of p53 wild-type and null isogenic colorectal cancer cell lines resistant to 5-Fluorouracil, oxaliplatin, and irinotecan. *Clin Cancer Res* 2004;10:2158–2167.
 26. Yoshikawa R, Kusunoki M, Yanagi H, Noda M, Furuyama J, Yamamura T, Hashimoto-Tamaoki T. Dual antitumor effects of 5-Fluorouracil on the cell cycle in colorectal carcinoma cells: a novel target mechanism concept for pharmacokinetic modulating chemotherapy. *Cancer Res* 2001;61:1029–1037.
 27. Leclerc E, David B, Griscom L, Lepioufle B, Fujii T, Layrolle P, Legallais C. Study of osteoblastic cells in a microfluidic environment. *Biomaterials* 2006;27:586–595.
 28. Kelly JH. Permanent human hepatocyte cell line and its use in a liver assist device (LAD). US Pat., 5,290,684 (1994).
 29. Triglia D, Purchio A. Clonal cells and cell lines derived from C3A cells and methods of making and using them. US Pat., 6,653,105 (2003).
 30. Harker WG, MacKintosh FR, Sikic BI. Development and characterization of a human sarcoma cell line, MES-SA, sensitive to multiple drugs. *Cancer Res* 1983;43:4943–4950.
 31. Ruoslahti E. Stretching is good for a cell. *Science* 1997;276:1345–1346.
 32. Chen CS, Mrksich M, Huang S, Whitesides GM, Ingber DE. Micropatterned surfaces for control of cell shape, position, and function. *Biotechnol Prog* 1998;14:356–363.
 33. Prokop A, Prokop Z, Schaffer D, Kozlov E, Wikswo J, Cliffl D, Baudenbacher F. NanoLiterBioReactor: Long-term mammalian cell culture at nanofabricated scale. *Biomed Microdevices* 2004;6:325–339.